Preprints of the 19th World Congress
The International Federation of Automatic Control
Cape Town, South Africa. August 24-29, 2014

Computing Instantaneous Throughput For Spatially Constrained Aiming Tasks

Jeffrey N. Shelton * **George T.C.Chiu** **

* *School of Mechanical Engineering, Purdue University, West Lafayette, IN 47907 USA (e-mail: shelton@purdue.edu).*
** *School of Mechanical Engineering, Purdue University, West Lafayette, IN 47907 USA (e-mail: gchiu@purdue.edu).*

Abstract: Motor throughput is a standard measure of how rapidly information can be transmitted through an input device (such as a mouse or wand) by a human user carrying out point-to-point movement (also known as a Fitts' task.) As low-cost motion tracking systems become more prevalent, engineers are presented with increasing opportunities to control operations using hand gestures. However, accurate analysis of motor throughput in such cases may be difficult, as muscle tremors may prevent midair motions from coming to an absolute stop, and visual obstructions may prevent endpoint data from being reliably captured. A lack of accurate temporal and spatial endpoint information precludes any determination of motor throughput. Inspired by Fitts' information channel model, we derive a measure of *instantaneous* motor throughput. Observation of this instantaneous measure demonstrates how the traditional measure of information bandwidth, Fitts' motor throughput, emerges during the course of an aimed movement. Further, an experimental study demonstrates that instantaneous throughput (ITP) profiles exhibit a common shape when plotted against normalized distance. We select the moment of peak variance to be the most convenient landmark along the ITP trajectory for computing an overall throughput value, and demonstrate that this new method compares favorably with traditional throughput measures.

Keywords: Human factors, Information flow, Physiological models, Positional variance, Fitts' hypothesis

1. INTRODUCTION

With the advent of low-cost tracking systems, a number of new control challenges related to human gesturing are becoming evident. Mid-air movements of the hand and arm may be used to interact with large-screen displays (Baudisch, 2006), move objects in virtual environments (Liu et al., 2011), or teleoperate remote robots (Eliav et al., 2011); all areas of potential interest to control engineers. However, much of the literature related to pointing and gesturing is associated with research into human-computer interfaces (HCI). A standard practice of the HCI field (Zhai, 2004) is to express the effectiveness of a particular gesture or pointing device in terms of "information throughput."

For those in the control community, the notion of associating "information" with a moving body's trajectory may seem a bit unusual. This interpretation results from the seminal work of Fitts (1954). Inspired by Shannon's information theory (Shannon and Weaver, 1949), Fitts assigned an informational value (measured in bits) to aiming tasks of varying relative precision. He defined the *index of difficulty* for a movement to be

$$ID_{\text{Fitts}} = \log_2 \left(\frac{2D}{W} \right) , \tag{1}$$

where D is the movement distance (or amplitude), and W is the target width. (We use the subscript to denote Fitts' original definition for task difficulty; a slightly modified definition will be introduced shortly.) He further defined an *index of performance* (IP) to capture the *mean* rate of movement information transfer, which he expressed as

$$IP = \frac{ID_{\text{Fitts}}}{MT} , \tag{2}$$

with MT representing mean movement time. This measure, also referred to as *throughput*, blends the performance elements of speed and accuracy into a single parameter that can be compared across differing task configurations. Relying on experimental data, Fitts found the human motor system to behave as a bandwidth-limited information channel, constrained in the amount of movement "information" it can process per a given time unit. His notion of an upper bound on the information processing rate is herein referred to as the *motor channel hypothesis*.

Although the communication analogy used by Fitts to describe motor behavior is conceptually informative, it must be acknowledged that applying information theory to motor control is potentially confusing. Any bridge between Fitts' ID parameter and Shannon's definition of information is tenuous at best. Unlike new data flowing into Shannon's information channel, the position and velocity of a rigid limb cannot instantaneously change. Although we follow convention in referring to the ID term as an information measure, Fitts' appropriation of information theory terminology is to be considered descriptive, rather than explanatory (Baird, 1984). Reviews of HCI research utilizing Fitts' motor channel hypothesis can be found in MacKenzie (1992) and Seow (2005). This paper attempts to explain Fitts' notion of information throughput in terms of movement kinematics. This is accomplished by introducing the concept of *instantaneous throughput* (ITP).

2. MEASURING MOVEMENT INFORMATION

Throughput, as defined in (2), expresses the average rate at which movement information is transmitted. Fitts found throughput to remain "approximately constant over a considerable range of movement amplitudes and tolerance limits." He theorized, therefore, that the rate of motor information transfer is independent of task configuration.

Although Fitts' *ID* measure is widely accepted, many researchers have proposed alternate definitions that better agree with experimental data (Plamondon and Alimi, 1997). A particular shortcoming of Fitts' definition is that his index of difficulty turns negative as D approaches zero from above. One of the most widely-used alternative definitions (Soukoreff and MacKenzie, 2004; Zhai, 2004; Seow, 2005) is the "Shannon" formulation, so named because it takes on a algebraic form that is similar to Theorem 17 in Shannon and Weaver (1949). First proposed by MacKenzie (1989), this formulation holds that

$$ID = \log_2\left(\frac{D}{W} + 1\right). \tag{3}$$

While this measure is always non-negative, the smallest achievable ratio of $^D/_W$ is $^1/_2$ when the target is centered on its own width and $W > 0$. We thus note a practical lower bound of 0.585 on the Shannon formulation for *ID*. Since the mathematical development shown below benefits from a non-negative *ID*, the Shannon formulation of (3) is used hereafter in this paper.

2.1 Effective motor information

Subjects carrying out repeated aiming or pointing trials are usually unable to match their mean endpoint to the target center. Additionally, they fail to distribute their endpoints across the entire target width, either clustering their endpoints too narrowly, or spreading their endpoints beyond the target region (Zhai et al., 2004). This results in a transfer of more or less information than is required by the nominal task configuration (Soukoreff and MacKenzie, 2004). To compensate for the difference between nominal and actual information transfers, motor information values are often computed using measures for *effective distance* (D_e) and *effective target width* (W_e). Effective distance is the mean distance traveled for an ensemble of trials, while the effective target width is frequently computed as

$$W_e = 4.133 \cdot s\left(D_f\right), \tag{4}$$

where $s\left(D_f\right)$ is the sample standard deviation of the movement endpoints. The factor of 4.133 derives from the maximal entropy associated with a one-dimensional Gaussian distribution (Shannon and Weaver, 1949, p. 56). Since subjects distribute their endpoints in an approximately normal manner (Crossman, 1960; Fitts and Radford, 1966), W_e also provides an estimate of how wide a target is required to ensure that 96% of all movements terminate within the target bounds. Matching the algebraic form of (3), an *effective index of difficulty* can be defined as

$$ID_e = \log_2\left(\frac{D_e}{W_e} + 1\right). \tag{5}$$

This results in an *effective throughput* of

$$IP_e = \frac{ID_e}{MT}. \tag{6}$$

2.2 Instantaneous throughput

This study proposes an *instantaneous* rate of information transfer, analogous to Fitts' mean rate. Consider an ensemble of $n > 1$ trials. Let $I(t)$ represent all information transmitted by the ensemble between times t_0 and $t > t_0$, with each trial starting at t_0. Since information flow is associated with limb movement, and such movements are limited in size and speed, we assume $I(t)$ to be continuous and finite, with an initial value of $I(t_0) = 0$. There must exist, therefore, some *instantaneous throughput* function, $\phi(t)$, whereby

$$I(t) = \int_{t_0}^{t} \phi(\tau)\, d\tau. \tag{7}$$

Information is to be transmitted as quickly as possible in rapid movement, making any reversal in the direction of information flow counterproductive. We thus assume that both $I(t)$ and $\phi(t)$ are uniformly non-negative, such that

$$\phi(t) \begin{cases} = 0, \ t < t_0 \\ \geq 0, \ t \geq t_0 \end{cases}. \tag{8}$$

Once movement is initiated, additional information continues to be delivered as long as at least one trial from the ensemble remains in motion. Let δ_k represent the instant at which the k^{th} trial is completed, where $k = \{1 \ldots n\}$. Information ceases to be conveyed when $t \geq \max\{\delta_k\} = \delta_{\max}$; that is, when all endpoint data has been established. We assume that ID_e, as defined in (5), captures all motor information delivered via limb motion.

2.3 Computing instantaneous throughput

When all ensemble movement is completed, $I(\delta_{\max}) = ID_e$. For this reason, we let $I(t)$ assume the algebraic form shown for ID_e in (5), while maintaining the relationship of (7). Thus, we let

$$\phi(t) = \frac{dI(t)}{dt} = \frac{d}{dt}\left[\log_2\left(\frac{\theta(t)}{\omega(t)} + 1\right)\right], \tag{9}$$

where $\theta(t)$ and $\omega(t)$ are the *instantaneous effective position* and *instantaneous effective position spread.* Let $\theta(t)$ be equal to the mean ensemble position at time t, while $\omega(t) = 4.133 \cdot s(t)$, with $s(t)$ representing the coincident sample standard deviation for the ensemble. Since movement data is usually sampled at discrete instances, the above equations are next converted to a discrete form.

We assume position data is gathered during n trials of a common task. These samples, are collected at intervals of duration Δ. Each trial is retrospectively synchronized to begin at time $t = 0$. Next, values for mean position and sample standard deviation are calculated at each sample index. Allow $j = 1, 2, \ldots, n$ to track the trial number, and $k = 0, 1, \ldots, N$ to identify the sample index, with $N = \lceil \delta_{\max}/\Delta \rceil$. Let $d(j, k)$ represent the position

Config.	Distance (deg)	Target Width (deg)	Nominal Fitts *ID*	Nominal Shannon *ID*
1	15	5	2.58	2.00
2	15	2.5	3.58	2.81
3	30	5	3.58	2.81
4	15	1.25	4.58	3.70
5	30	2.5	4.58	3.70
6	60	5	4.58	3.70
7	30	1.25	5.58	4.64
8	60	2.5	5.58	4.64
9	60	1.25	6.58	5.61

Table 1. Experimental task configurations for targeted forearm movement.

of trial j at time index k, with $d(j,0) = 0$. Then the *discrete instantaneous effective position* for sample index k is denoted as

$$\Theta(k) = \frac{1}{n}\sum_{j=1}^{n} d(j,k). \tag{10}$$

A *discrete instantaneous effective position spread* at sample index k is defined as

$$\Omega(k) = 4.133 \cdot s(k)\,, \tag{11}$$

where $s(k)$ is the sample standard deviation of the n position values measured at time $t = k\Delta$. Let $\mathcal{D}_k$ denote numerical differentiation with respect to index k, and allow $I(k)$ to be discrete samples of $I(t)$ at times $t = k\Delta$. Following the structure of (9), it is possible to define the rate of change in movement information at sample index k as

$$\Phi(k) = \mathcal{D}_k\left\{I(k)\right\} = \mathcal{D}_k\left\{\log_2\left(\frac{\Theta(k)}{\Omega(k)} + 1\right)\right\}\,, \tag{12}$$

with $\Phi(k)$ being deemed the *discrete instantaneous throughput* for a movement ensemble.

3. EXPERIMENTAL METHOD

Seven subjects (six male and one female) with no known neurological deficits participated in this experiment. Informed consent was given by each subject prior to entering the study, and none of the subjects were paid for their participation. As self-reported, one subject was left-handed, while the remainder were right-hand dominant. All subjects were required to use their right arm in performing aimed movement tasks. Subsequent reference to the seven subjects is notated as S1 through S7.

3.1 Experimental setup

A freely rotating mechanical swing arm was attached to a large wooden desk. Each subject placed their right forearm atop the swing arm, with the knob of their right elbow located on a rubber grommet centered on the vertical pivot axis. Subjects were seated such that their right elbow was horizontally aligned with the right shoulder, effectively tying rotation of the test fixture swing arm to a subject's right forearm movement about the elbow joint.

Beginning with the swing arm abutting a vertical start post, a single task trial consisted of having the subject rotate their forearm, while grasping the swing arm handle, away from their body until a pointer at the end of the mechanical arm was positioned in front of, and inside the width of, a vertical target. Multiple trials were made in each of nine task configurations, detailed in Table 1. Test sessions were segmented into two halves. During each half, subjects ran 30 trials in each of the nine task configurations, which took place in a random sequence that was different for each subject.

3.2 Data acquisition

A BEI (Goleta, CA, USA) Model HS-25 Incremental Encoder, having a resolution of 3600 cycles per turn, was used to measure swing arm rotational position. This data was stored using a US Digital (Vancouver, WA, USA) Model USB4 Encoder Acquisition Device, which kept track of the cumulative position count, storing data at a sampling rate of 500 Hz. Accelerative data was captured using a capacitive triaxial accelerometer, Model 3713 from PCB Piezotronics (Depew, NY, USA), with a sensing range of ± 20 g. Both rotary encoder and accelerometer signals were filtered offline using a 9th-order Butterworth lowpass filter with a cutoff frequency of 18 Hz. Velocity values were produced by cumulatively summing acceleration data for each trial, after offsetting the acceleration data to have zero mean. The resulting velocity traces were found to closely match those obtained by differentiating position data.

4. RESULTS

Oscillations due to muscle tremor remained evident in the position data at the beginning and end of each trial. It was therefore necessary to algorithmically determine the instances of movement initiation and cessation. Each movement was deemed to start 30 ms after its acceleration turned uniformly positive, in advance of reaching an accelerative maximum. As acceleration passes from negative to positive, limb velocity is necessarily at a local minimum. Thus, all movements were aligned near this kinematic roadmark, but were then given an additional 30 ms to return to a velocity of approximately zero. Each trial was were declared complete when the rate of rotation slowed to $6.5°$ per second and stayed below that velocity for at least 200 ms. Unpaired two-sampled t-tests were used to check for learning effects; only one subject in a single configuration was faster during the first five trials of the second block, as compared to the first five trials of the first block. Hence, no substantive learning effect was detected.

4.1 Instantaneous throughput (ITP) profiles

Estimates of instantaneous throughput were calculated, in accordance with (12), at 2 ms intervals for all seven subjects in each of nine task configurations. Values for instantaneous throughput $\Phi(k)$ were obtained by passing $I(k)$ data through a low-pass (18 Hz) differentiating filter. Results for S3, who posted the median movement time, are displayed in Fig. 1(a). Previous studies have shown positional variance in aiming tasks to display a single bell-shaped peak centered in the middle of the movement (Todorov et al., 2005; Selen et al., 2006). Thus, points of peak positional variance are easy to extract from

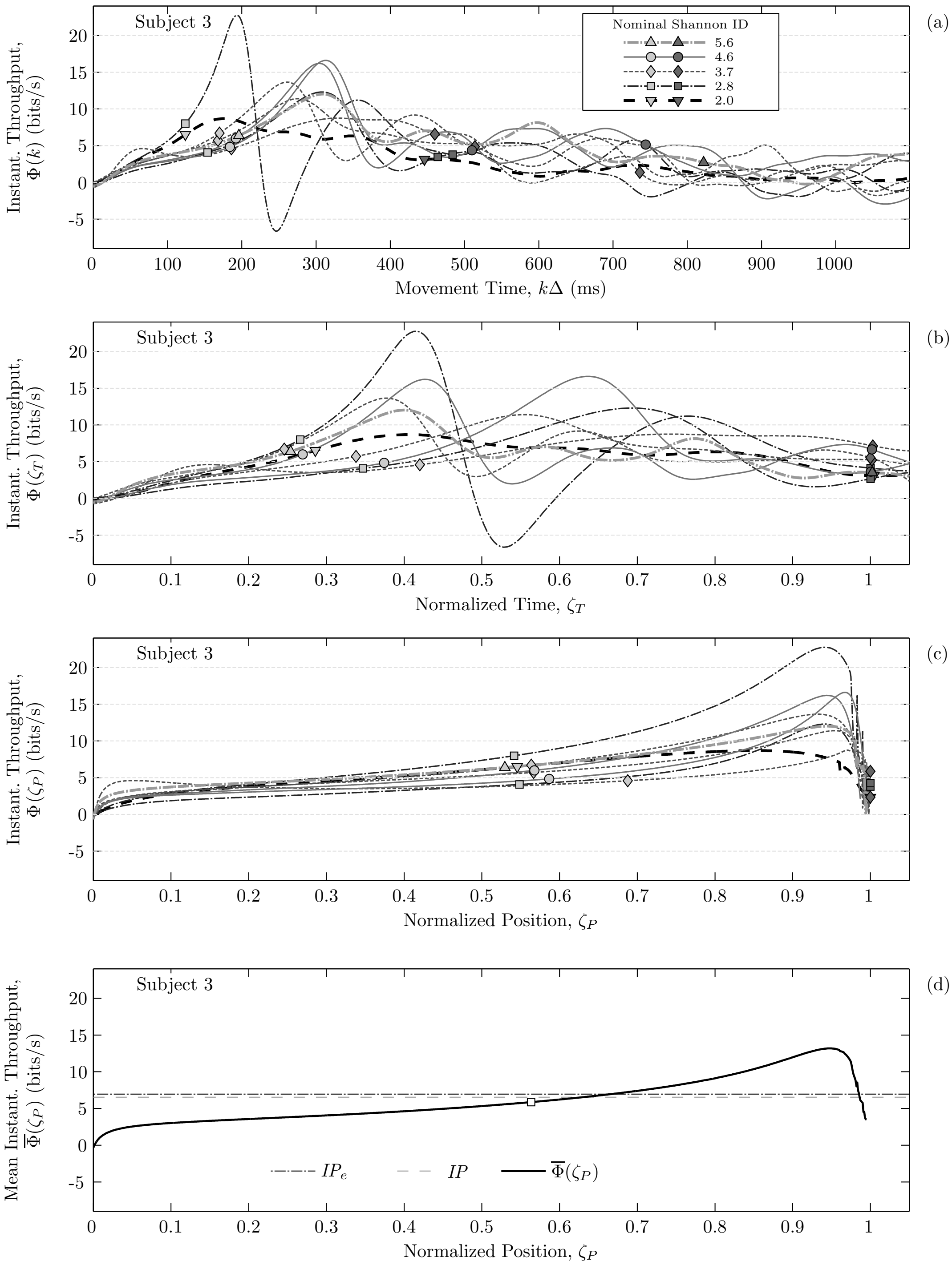

Fig. 1. Progression of instantaneous throughput in each of nine task configurations. Leading markers (light gray) indicate points of peak positional variance, while trailing markers (dark gray) denote algorithmically-determined instances of movement termination. ITP is plotted against movement time in (a), against normalized time in (b), and against normalized movement distance in (c). Averaging the nine ITP curves from (c) produces the solid black trace shown in (d). The square marker identifies the point of peak variance. Conventional measures of throughput, IP and IP_e are shown as horizontal lines.

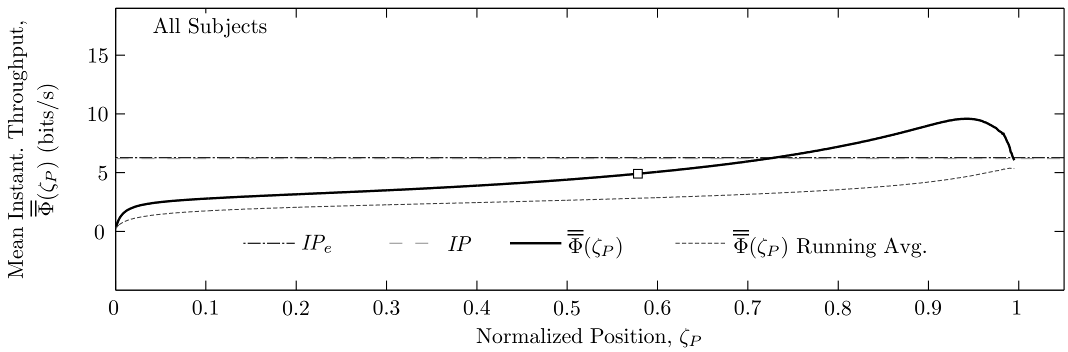

Fig. 2. Average of mean ITP curves across all seven subjects. The square white marker indicates the mean peak variance ITP, also notated as IP_i. A running average of the $\overline{\overline{\Phi}}(\zeta_P)$ curve is shown as a dashed line.

kinematic data, and are denoted in Fig. 1(a) by the leading light gray markers. Trailing dark gray markers indicate the mean times of movement cessation in each of the nine test configurations. Declines in ITP, evident beyond the trailing markers, occur as slower-than-average trials move into the target zone, thereby reducing positional spread.

Although ITP curves should theoretically start from zero, seven of the nine traces in Fig. 1(a) begin with slightly negative values. This situation stems from allowing subjects to initiate movement from non-stationary states, and thus having to algorithmically approximate (as described above) a stationary start. After 15 ms, all nine configuration traces turn positive. Negative ITP values can also be seen later in the movements; as will be shown, this is an indicator that the movement is nearing its endpoint.

Beyond 100 ms, the configuration trajectories of Fig. 1(a) begin to diverge; the only significant similarity becomes a slow oscillatory decline toward zero as movement time increases. However, considering the possibility of proportional timing, these curves are plotted against normalized time in Fig. 1(b). Again, there doesn't seem to be a great deal of commonality in the time-normalized ITP profiles beyond the first third of the movement. We next examined the ITP curves as functions of normalized position, as shown in Fig. 1(c). This graph significantly skews the data at movement initiation, pushing the initial ITP spikes to the far left edge, since they occur while limb velocity is just beginning to climb, and limb displacement remains near zero. All ITP oscillations taking place beyond 300 ms are pushed to the far right edge, as the movements are substantially complete after the first quarter-second of movement time.

Although they are not identical, there is a noticeable uniformity to the configuration ITP profiles seen in panel (c). Each ITP curve rises smoothly from zero toward a maximum that occurs near $\zeta_P = 0.95$. A rise of more than 22 bits/s is evident for S3 in the top trace of panel (c), indicating a substantive change in ITP during the ensemble movement. All seven subjects revealed this type of positive incline, with the level of instantaneous throughput rising as the movement proceeds. During the movement, the spread of ITP values, from the lowest starting value to the highest peak value, across all nine configurations for each of the seven subjects was, respectively: 13.92, 13.82, 23.47, 10.54, 12.91, 29.29, and 10.26 bits/s. This indicates that the average incline seen for S3 is steeper, by a nearly 2:1 margin, than that for 5 of the remaining 6 subjects. To provide a gauge of mid-movement spread, the standard deviations of each subject's ITP values, at points of peak variance, were, respectively: 0.75, 0.62, 1.22, 0.36, 1.25, 1.07, and 0.46 bits/s. Thus, when compared to the other six subjects, S3 produced one of the steepest inclines, and the largest separation between individual IPT traces. Traces for remaining subjects are mostly flatter and more tightly clustered.

Averaging the nine traces of Fig. 1(c), with respect to normalized position, produces the solid black line shown in Fig. 1(d). The white marker identifies the mean peak variance value of 6.64 bits/s, which was computed by taking the average peak variance values, $\Phi(k_{\text{pv}})$, for the nine task configurations. For reference, conventional measures of IP and IP_e are shown as horizontal lines.

Calculating an overall mean ITP for all seven subjects produces the curve shown in Fig. 2. The mean peak variance ITP of 5.51 bits/s is identified by the white square marker. For comparison, the IP_e value is 6.29, while IP is 6.18 bits/s. Examination of similar data gathered for an as-yet-unpublished study (collected under the same test protocol, but using lower task difficulties), indicates that the point of mean peak variance ITP may lie above the IP_e line, as well as below it. The notation IP_i is hereafter used in referring to this peak variance point, which we call the *peak variance instantaneous throughput*.

4.2 Effective throughput

Based on the ITP definition, we expect $I(t)/t$ to approximate IP_e for $t \geq \delta_{\max}$. Let the running average of $\phi(t)$ with respect to t be denoted as $\overline{T}(t)$. Since $\phi(t)$ was defined as being uniformly non-negative, so is $\overline{T}(t)$. Average ITP as movement concludes is

$$\overline{T}\left(\delta_{\max}\right) = \frac{ID_e}{\delta_{\max}}. \tag{13}$$

If all movements in the ensemble are of the same duration, then $MT = \delta_{k=1\ldots n} = \delta_{\max}$, and $\overline{T}(\delta_{\max}) = IP_e$. However, when multiple trials from an ensemble have unequal temporal lengths, the mean movement time is less than the maximum trial duration; $MT < \delta_{\max}$. Therefore, the traditional index of performance is greater than terminal value of the ITP running average, as

$$\overline{T}\,(\delta_{\max}) = \frac{I(\delta_{\max})}{\delta_{\max}} = \frac{ID_e}{\delta_{\max}} < \frac{ID_e}{MT} = IP_e \qquad (14)$$

This effect can be seen in Fig. 2, where the running average is less than IP_e as the movement concludes. The extent of this inequality depends, of course, on the difference between MT and $\delta_{\max}$. The standard deviation of the IP_e values gathered in this study was 1.45 bits/s, while the standard deviation of the $\Phi(k_{\text{pv}})$ values (that went into the computation of IP_i) was 1.51 bits/s. Thus, there is a similar spread in these two throughput measures.

5. DISCUSSION

This study examines only "unfinished" movements; that is, movements that do not come to complete stops. Once inside the target region, subjects continued to exhibit slight movement tremors. Thus, the IP_e values in this study are based on algorithmically-determined movement durations and endpoint locations. Since IP_e is used as a reference for evaluating the validity of IP_i values, a future investigation needs to compare the IP_e and IP_i values for a discrete aiming task in which all movements halt fully. Nonetheless, a method has been shown for determining motor information throughput in the absence of temporal or spatial knowledge of aimed movement endpoints, thus providing an alternate computation of motor throughput in situations where in-situ measurements of endpoint data cannot be gathered.

5.1 Relationship to Fitts' motor channel hypothesis

Fitts' speculated that mean movement throughput was constant for all aiming movements of a given type, regardless of task configuration. The least complicated means for achieving this end, absent all other physiological objectives and constraints, would be for the ITP to remain constant throughout the movement. Prior studies have not investigated throughput on a continuous basis, as established throughput definitions considered only the *mean* rate of information flow. This hurdle is eliminated with a definition for measuring throughput on an instantaneous basis.

Our experimental data indicates that the ITP varies significantly as the movement progresses. Nonetheless, ITP curves take on a common shape when plotted against normalized position. Thus, Fitts' hypothesis can be explained in terms of kinematic similarities. While the relationship between distance traveled and spatial variance is common across tasks of varying difficulty with respect to normalized distance, the information flow is certainly not constant. This understanding serves to remove some of the mystery from Fitts' notion of "motor information."

5.2 Conclusion

A method for determining aimed movement throughput without endpoint data has been described. Experimental data suggests that this method produces results that are comparable with traditional measures requiring temporal and spatial knowledge of movement endpoints. This methodology also suggests that Fitts' motor hypothesis is due to kinematic similarities in discrete aiming tasks, rather than an ongoing regulation of motor information throughput. Alignment of ITP curves on a normalized-displacement basis suggests that further research needs to be conducted into how the body might regulate movement via displacement-based, rather than time-based, control methods.

REFERENCES

Baird, J. (1984). Information-theory and information-processing. *Information Processing & Management*, 20(3), 373–381.

Baudisch, P. (2006). Interacting with large displays. *Computer*, 39(4), 96–97.

Crossman, E.R.F.W. (1960). The information-capacity of the human motor-system in pursuit tracking. *Quarterly Journal of Experimental Psychology*, 12(1), 1–16.

Eliav, A., Lavie, T., Parmet, Y., Stern, H., and Edan, Y. (2011). Advanced methods for displays and remote control of robots. *Applied ergonomics*, 42(6), 820–829.

Fitts, P.M. and Radford, B.K. (1966). Information capacity of discrete motor responses under different cognitive sets. *Journal of Experimental Psychology*, 71(4), 475–&.

Fitts, P.M. (1954). The information capacity of the human motor system in controlling the amplitude of movement. *Journal of Experimental Psychology*, 47, 381–391.

Liu, L., Martens, J.B., and van Liere, R. (2011). Revisiting path steering for 3D manipulation tasks. *international Journal of Human-computer Studies*, 69(3), 170–181.

MacKenzie, I.S. (1989). A note on the information-theoretic basis for Fitts law. *Journal of Motor Behavior*, 21(3), 323–330.

MacKenzie, I. (1992). Fitts' law as a research and design tool in human-computer interaction. *Human-Computer Interaction*, 7, 91–139.

Plamondon, R. and Alimi, A.M. (1997). Speed/accuracy trade-offs in target-directed movements. *Behavioral and Brain Sciences*, 20, 279–349.

Selen, L.P.J., Beek, P.J., and van Dieen, J.H. (2006). Impedance is modulated to meet accuracy demands during goal-directed arm movements. *Experimental Brain Research*, 172(1), 129–138.

Seow, S.C. (2005). Information theoretic models of HCI: A comparison of the Hick-Hyman law and Fitts' law. *Human-computer Interaction*, 20(3), 315–352.

Shannon, C.E. and Weaver, W. (1949). *The Mathematical Theory of Communication*. University of Illinois Press.

Soukoreff, R.W. and MacKenzie, I.S. (2004). Towards a standard for pointing device evaluation, perspectives on 27 years of Fitts' law research in HCI. *International Journal of Human-computer Studies*, 61(6), 751–789.

Todorov, E., Li, W.W., and Pan, X.C. (2005). From task parameters to motor synergies: A hierarchical framework for approximately optimal control of redundant manipulators. *Journal Of Robotic Systems*, 22(11), 691–710.

Zhai, S.M. (2004). Characterizing computer input with Fitts' law parameters - the information and non-information aspects of pointing. *International Journal of Human-Computer Studies*, 61(6), 791–809.

Zhai, S.M., Kong, J., and Ren, X.S. (2004). Speed-accuracy tradeoff in Fitts' law tasks - on the equivalency of actual and nominal pointing precision. *International Journal of Human-Computer Studies*, 61(6), 823–856.